Supplemental Data

to

Leucine/Valine Residues Direct Oxygenation of Linoleic Acid by (10*R*)- and (8*R*)-Dioxygenases. EXPRESSION AND SITE-DIRECTED MUTAGENESIS OF (10*R*)-DIOXYGENASE WITH EPOXYALCOHOL SYNTHASE ACTIVITY

by

Ulrike Garscha and Ernst H. Oliw

1. Gene cloning of 10*R*-DOX

The intron-exon borders were identified as summarized in Table 1S by comparison of the published genomic sequence with the cDNA sequence (GenBank Accession Nr. ACL14177).

Table 1S. Overview of the intron-exons of the 10*R*-DOX gene

Exons	mRNA nucleotides	Intron borders	Intron size (bp)
Exon 1	1-420	gtaag... ...tag	70
Exon 2	421-518	gtgag... ...tag	56
Exon 3	519- 760	gtatg... ...cag	54
Exon 4	761-965	gtcca... ...tag	55
Exon 5	966-1106	gtacg... ...tag	63
Exon 6	1107-1197	gtaag... ...cag	53
Exon 7	1198-1528	gtgag... ...aag	61
Exon 8	1529-1872	gtaag... ...cag	57
Exon 9	1873-2405	gtgag... ...cag	54
Exon 10	2406-2820	gtaag... ...tag	61
Exon 11	2821-3060	gtacg... ...tag	59
Exon 12	3061-3338	gtgag... ...cag	53
Exon 13	3338-3366		

Nucleotides are numbered from A[1]TG, yielding an open reading frame of 3366-bp, including the stop codon, and a corresponding gene sequence of 4062-bp. The deduced primary amino acid sequence of 10*R*-DOX suggested a molecular weight of 126.5 kDa.

2. Alignments

An alignment of 10*R*-DOX of *A. fumigatus* (GenBank Accession No. ACL14177) and 7,8-LDS of *G. graminis* (GenBank Accession No. AF124979) is shown in Fig. 1S.

```
  1  M L R R F S S T F K K K G D R E S K Q N G T A S S S S A A V  10-DOX_Af
  1  - - - - - - - - - - - - - - - - - - - - - - - - - - - M T  7,8-LDS-Gg

 31  A N T N N N D N K R H S K I S A A R K S S S D D D R N E K K  10-DOX_Af
  3  V S T H H D D - - - - - - - S P G L S G R L R D L L H H V F  7,8-LDS-Gg

 61  G N S V S P F E K Y A S V L H A S R S P I P N Q T G D G A Y  10-DOX_Af
 26  G N Q K S P - T V Y P N A P G N S A K P V P - - - - - - - -  7,8-LDS-Gg

 91  L E H E H T T S L L Q D A R H L G F K D F K T L K E V I E S  10-DOX_Af
```

```
 47  - - - - - - T G L A D D I D K L G F K D I D T L L I F L N S  7,8-LDS-Gg

121  K L P G G Q L I D D K T M L M E R I I Q L V S R L P H N S K  10-DOX_Af
 71  A V K G - - V N D D Q Q F L L E K M I Q L L A K L P P A S R  7,8-LDS-Gg

151  H R E E L T N A F L T E L W D S L P H P P L S Y M G N D Y A  10-DOX_Af
 99  E G K K L T D G L I N D L W D S L D H P P V A S L G K G F S  7,8-LDS-Gg

181  Y R S A D G S N N N P T L P R L G A A N T L Y A R T I P P L  10-DOX_Af
129  F R E P D G S N N N I H L P S L G A A N T P Y A R S T K P L  7,8-LDS-Gg

211  I I Q P G G L P D P G L V F D T L F A R - - Q T F K P H P N  10-DOX_Af
159  V F Q N P N P P D P A T I F D T L M V R D P A K F R P H P N  7,8-LDS-Gg

239  K V S S V F F Y W A S L I I H D I F Q T D Y K N P N M N K T  10-DOX_Af
189  K I S S M L F Y L A T I I T H D I F Q T S P R D F N I N L T  7,8-LDS-Gg

269  S G Y L D L S I L Y G D V Q E E Q N L I R T F K D G K L K P  10-DOX_Af
219  S S Y L D L S P L Y G R N H D E Q M A V R T G K D G L L K P  7,8-LDS-Gg

299  D S F S E P R L Q A F P A T C C V L M V M L N R F H N Y A V  10-DOX_Af
249  D T F S S K R V I G F P P G V G A F L I M F N R F H N Y V V  7,8-LDS-Gg

329  E Q L A A I N E N G R F T K P A D N L S E E E A K K A W A K  10-DOX_Af
279  T Q L A K I N E G G R F K R P T T - - - - P D D T A G W E T  7,8-LDS-Gg

359  Y D E D L F Q T G R L I T C G L Y I N I T L Y D Y L R T I V  10-DOX_Af
305  Y D N S L F Q T G R L I T C G L Y I N I V L G D Y V R T I L  7,8-LDS-Gg

389  N L N R T N S T W C L D P R A Q M E G - - - S H T A P S G L  10-DOX_Af
335  N L N R A N T T W N L D P R T K E G K S L L S K P T P E A V  7,8-LDS-Gg

416  G N Q C S V E F N L A Y R W H S A T S A T D E K W T E D V Y  10-DOX_Af
365  G N Q V S V E F N L I Y R W H C T I S E R D D K W T T N A M  7,8-LDS-Gg

446  - E R L M G K P A S E V S M T E L L M G L G K Y Q A E L P K  10-DOX_Af
395  R E A L G G Q D P A T A K M E D V M R A L G M F E K N I P D  7,8-LDS-Gg

475  D P S K R T F A D L E R Q A D G R F K D E D L V N L L V N A  10-DOX_Af
425  E P E K R T L A G L T R Q S D G A F D D T E L V K I L Q E S  7,8-LDS-Gg

505  V E D V A G S F G A R N V P K V L K N V E I L G I I Q S R K  10-DOX_Af
455  I E D V A G A F G P N H V P A C M R A I E I L G I K Q S R T  7,8-LDS-Gg

535  W N V G S L N E F R K F F G L K P Y E T F E E I N S D P D V  10-DOX_Af
485  W N V A T L N E F R Q F I G L T P H D S F Y H M N P D P K I  7,8-LDS-Gg

565  A E S L R S L Y D H P D F V E L Y P G I V A E E A K Q P M V  10-DOX_Af
515  C K I L A Q M Y D S P D A V E L Y P G I M A E A A K P P F S  7,8-LDS-Gg

595  P G V G I A P T Y T I S R A V L S D A V A L V R G D R F Y T  10-DOX_Af
545  P G S G L C P P Y T T S R A I L S D A V S L V R G D R F Y T  7,8-LDS-Gg

625  I D Y N P R N L T N W G Y S E V R Y D L S I N Q G C I F Y K  10-DOX_Af
575  V D Y T P R N I T N W G F N E A S T D K A V D W G H V I Y K  7,8-LDS-Gg

655  L A T R A F P N W F K P D S I Y A H Y P M T I P S E N R K I  10-DOX_Af
605  L F F R A F P N H F L P N S V Y A H F P F V V P S E N K L I  7,8-LDS-Gg

685  M K D L G R E I H Y S W D R P Q Y T P P R V D L V S Y S N A  10-DOX_Af
635  F E G L G A A N K Y S W D P P K A R A P I Q F I R S H K A V  7,8-LDS-Gg

715  K L V A E Q Q N Q F R A A W G D T V E F V F G K A S K E F K  10-DOX_Af
665  L E V L S N Q K D Y K V T W G P A I K M L S G D P A T S F A  7,8-LDS-Gg

745  L Y Q D S - A F I Q K H A D V M S K L L N K E E W H R S V K  10-DOX_Af
695  L A G D E P A N A A S R H H V I A A L T A P K Q W R D E V R  7,8-LDS-Gg

774  E F Y E D I T A K L L E D K T R R F G G I N - - - - - - Q V  10-DOX_Af
725  R F Y E V T T R D L L R R H G A P V H G V G A G P R T H E V  7,8-LDS-Gg
```

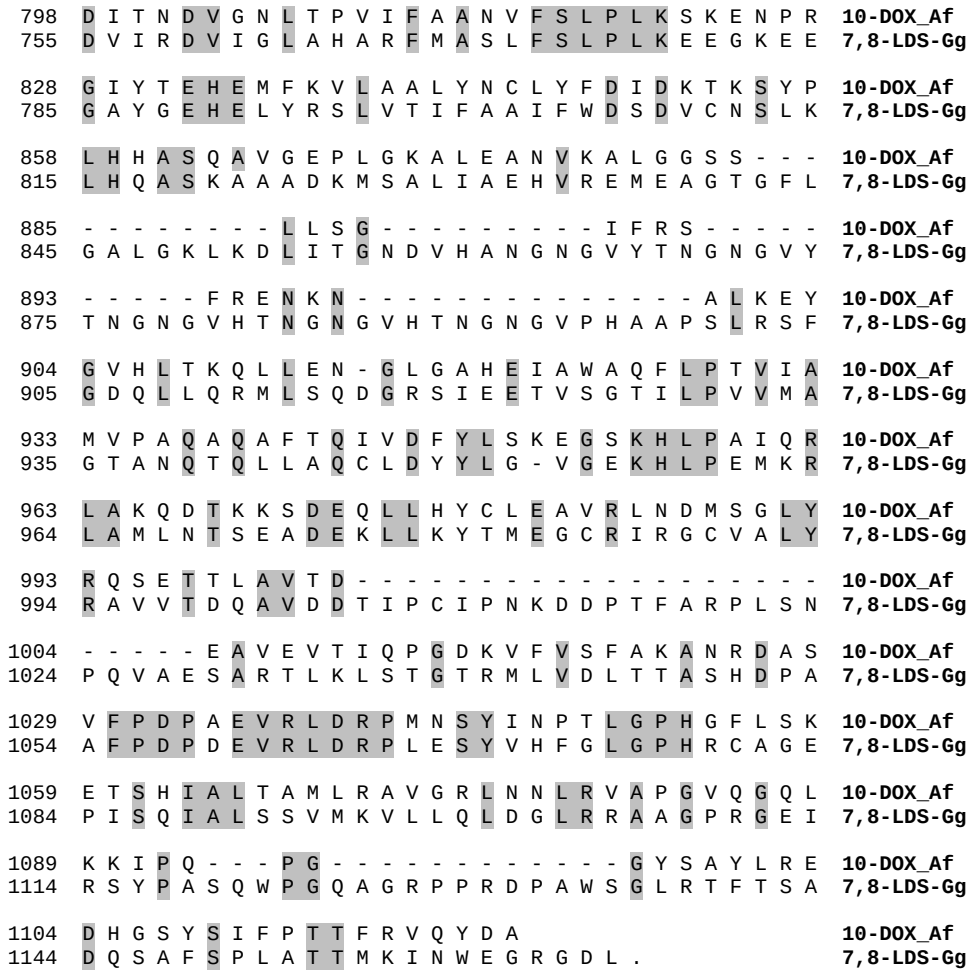

Fig. 1S. Alignment of 10*R*-DOX of *A. fumigatus* and 7,8-LDS of *G. graminis*. Identical residues are shaded grey. The ClustalW algorithm was used (DNA Star).

3. Expression of 10*R*-DOX

The open reading frame of 10*R*-DOX with its stop codon was ligated into pIZ/V5His between *Kpn*1 (ggtaccata A[1]TG TTG...) and *Xba*1 (GCC TAA[3366] gcatctttctaga..). This vector (pIZ_10-DOX) was used for site-directed mutagenesis.

pIZ_10-DOX was modified by insertion of a nucleotide (G) in front of the stop codon. The sequence now coded for a leucine residue after Ala[1121] in frame with the V5-His tag of pIZ/V5His. The C-terminal amino acid Ala[1121] was thus followed by 34 amino acids (Leu Ser Ile Phe Leu Glu Gly Pro Arg Phe Glu Gly Lys Pro Ile Pro Asn Pro Leu Leu Gly Leu Asp Ser Thr Arg Thr Gly His His His His His His). This vector (pIZ/V5His_10-DOX) was used to confirm protein expression and to assess expression levels by Western blot analysis.

4. Catalytic properties of recombinant 10*R*-DOX

4.1 Oxidation rate of 18:2n-6, time curve, and apparent Km

The oxidation rate of 18:2n-6 ranged from 0.15 to 0.8 nmol/min/ml lysate obtained from 1-2x10^{6}cells. The oxidation appeared to be linear for at least 30 min and the apparent K_m was estimated to be 50 μM (triplicate determinations), as shown in Fig. 2S.

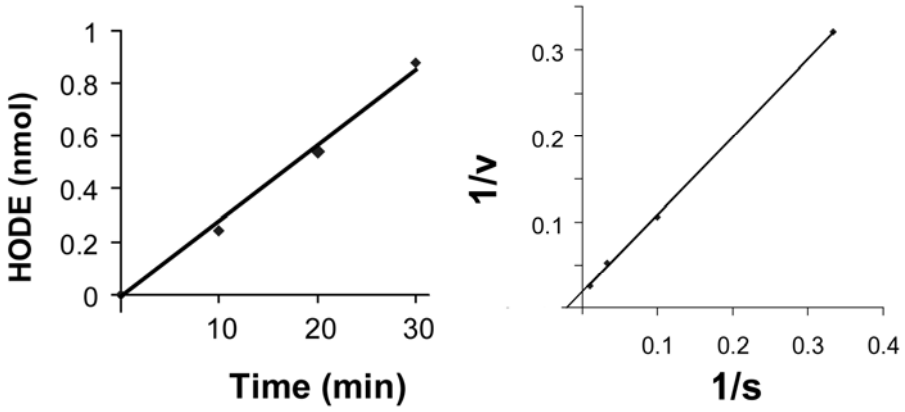

Fig. 2S. Time curve for oxidation of 18:2n-6 by recombinant 10*R*-DOX and an estimation of the apparent K_m by Lineweaver-Burke plot.

4.2 Oxygenation of 18:2n-6 to 12S(13R)epoxy-10R-hydroxy-18:1 and a comparison with oxygenation of vernolic acids

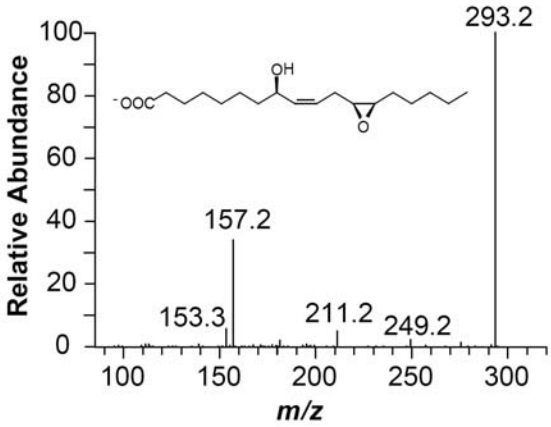

Fig. 3S. MS/MS spectrum (*m/z* 311→ full scan) of 8*R*-hydroxy-12(13)epoxy-9*Z*-18:1.

(+)Vernolic acid (12*S*(13*R*)epoxy-9*Z*-18:1) was transformed by 10*R*-DOX to 12*S*(13*R*)epoxy-8*R*-hydroxy-9*Z*-18:1 as the major product. This compound was identified by the MS/MS spectrum illustrated in Fig. 3S, which also was identical to the MS/MS spectra of the two isomers of 12(13)epoxy-8*R*-hydroxy-9*Z*-18:1, which were formed by epoxidation of 8*R*-HODE. 10*R*-DOX transformed 18:2n-6 to small amounts of 12*S*(13*R*)epoxy-10*R*-hydroxy-18:1, as outlined in Fig. 4S.

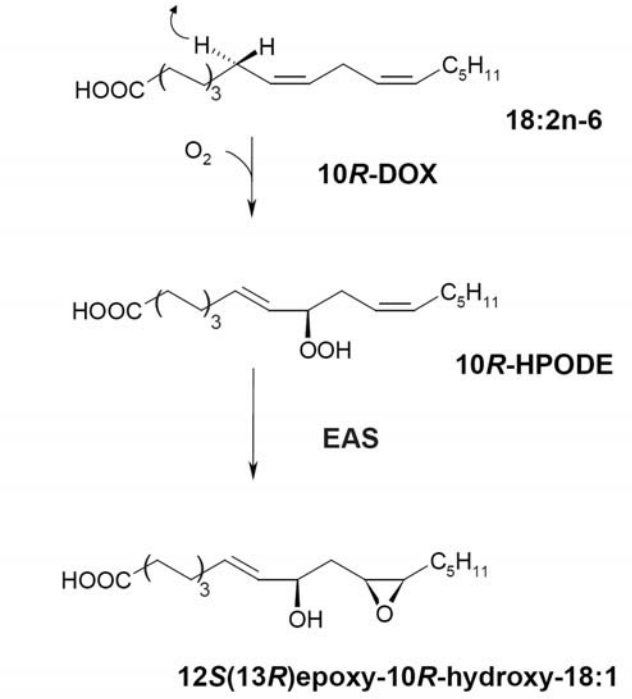

Fig. 4S. Summary of the oxygenation of 18:2n-6 by 10*R*-DOX with EAS activity. In addition, 10*R*-DOX may also form small amounts of racemic 8(9)epoxy-10*R*-hydroxy and 9(10)epoxy-8*R*-hydroxy-12*Z*-18:1 compounds.

4.3 Oxygenation of 18:2n-6 to 8(9)epoxy-10-hydroxy and 9(10)epoxy-8-hydroxy compounds

Due to Payne rearrangement, 8(9)epoxy-10-hydroxy and 9(10)epoxy-8-hydroxy compounds will give identical MS/MS spectra (32). These metabolites formed by 10*R*-DOX were separated by NP-HPLC into two pairs of isomers (Fig. 5S). The metabolites I and II were also formed by epoxidation of 10*R*-HODE and metabolites III and IV by epoxidation of 8*R*-HODE. Epoxidation of 10*S*- and 8*R*-HODE also yielded polar products, e.g., 12(13)epoxy-10-hydroxy- and 12(13)epoxy-8-hydroxy-18:1 compounds (not shown here).

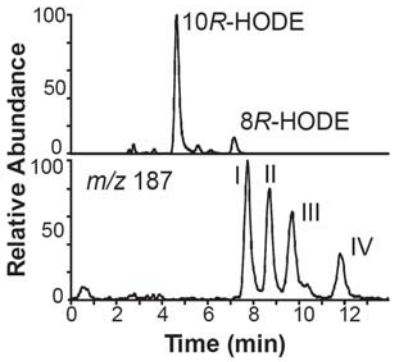

Fig. 5S. NP-HPLC analysis of major and minor metabolites formed from 18:2n-6 by 10*R*-DOX. Top trace, total ion current during MS/MS analysis (*m/z* 295→full scan) of hydroxy compounds. Bottom trace, MS/MS analysis (*m/z* 311 →full scan) with selective ion monitoring of *m/z* 187, a characteristic ion of 8(9)epoxy-10-hydroxy- and 9(10)epoxy-8-

hydroxy-12*Z*-18:1 compounds. Comparison with authentic standards suggested that peaks I and II contained 8(9)epoxy-10*R*-hydroxy-12*Z* -18:1 and peaks III and IV 9(10)epoxy-8*R*-hydroxy-12*Z*-18:1. All four metabolites have the same MS/MS spectra due to Payne rearrangement (32).

4.3 Oxygenation of 20:2n-6

10*R*-DOX transformed 20:2n-6 to a mixture of monohydroxy metabolites, as shown in Fig. 6S. The products were identified by their MS/MS spectra.

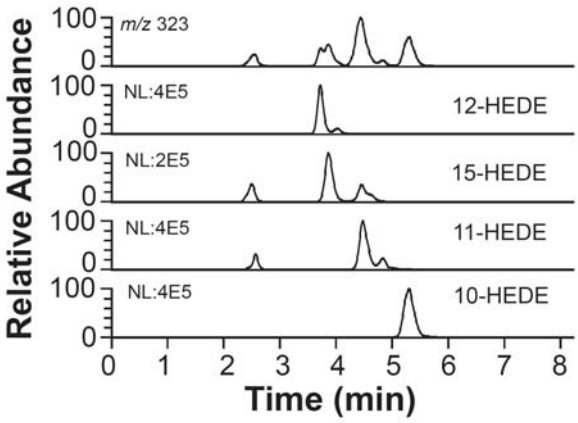

Fig. 6S. NP-HPLC-MS/MS analysis of HEDEs formed from 20:2n-6 by 10*R*-DOX. Top trace, total iron current of *m/z* 323 → full scan. The next four chromatograms show that 10-, 11-, 12-, and 15-HEDE were detected by MS/MS analysis monitoring characteristic ions (10-HEDE, *m/z* 185; 11-HEDE, *m/z* 199; 12-HEDE, *m/z* 211; 15-HEDE, *m/z* 223). The retention time and MS/MS spectra of the material eluting at 2.5 min were consistent with 14(15)epoxy- and 11(12)epoxy-18:1.

4.4 Oxygenation of 22:5n-6

2:5n-6 was a poor substrate of 10*R*-DOX, but RP-HPLC-MS/MS analysis suggested that small amounts of the bis-allylic hydroxy metabolite at the n-8 position might be formed (15-hydroxydocosapentaenoic acid; MS/MS m/z 345→full scan yielded characteristic signals at *m/z* 219 (cf. *m/z* 193 of 13-HETE) and *m/z* 275 (219-44)) might be formed, suggesting enzymatic transformation, along with the often non-enzymatically formed *cis-trans* conjugated products (Fig. 7). The transformation of 22:5n-6 was too low to merit further investigation.

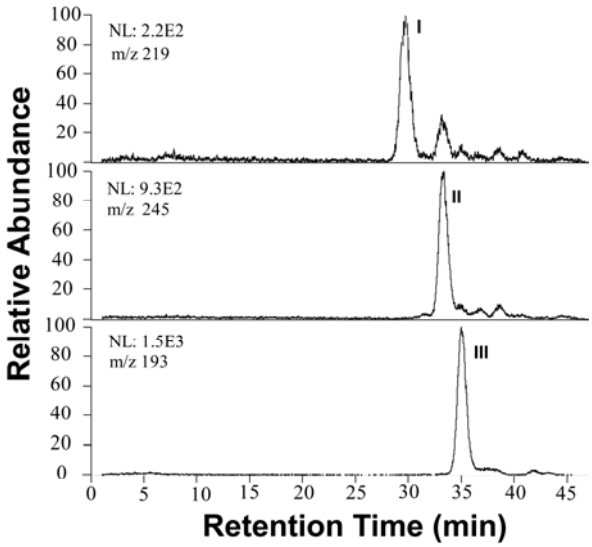

Fig. 7. RP-HPLC analysis of three hydroxylated metabolites of 22:5n-6 using gradient elution (from 75% to 80% methanol in 45 min at 0.3 ml/min). The MS/MS spectrum of the material in peak I was consistent with oxygenation at C-15 and the spectra of the material in peaks II and III with *cis-trans* conjugation of double bonds and oxygenation at C-17 and C-13, respectively.

4.3 Preparation of 13S-HETE by Mn-lipoxygenase

18:2n-6 is oxidized by Mn-lipoxygenase to 11*S*-HPODE and 13*R*-HPODE. 20:4n-6 was oxidized by Mn-lipoxygenase to 15*R*-HPETE and 13-HPETE (ref. (30)), and they were separated after reduction to alcohols by CP-HPLC on Reprosil Chiral-AM, as shown in Fig. 8S. On this column, the enantiomers of 13-HETE formed by 10*R*-DOX separated, and 13*S*-HETE eluted 2 min before 13*R*-HETE.

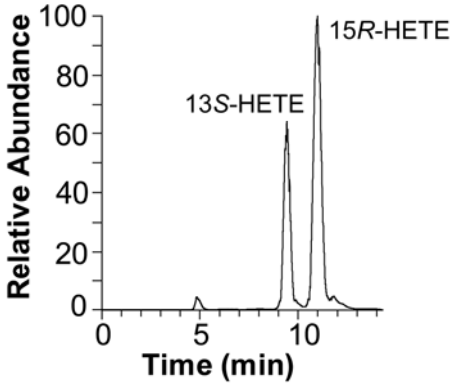

Fig. 8S. Separation of 15*R*-HETE and 13*S*-HETE formed by Mn-lipoxygenase by CP-HPLC and MS/MS analysis. The chromatogram shows the total ion current of MS/MS analysis of the carboxylate anions.

5. Biosynthesis of 8*R*-HODE and 10*R*-HODE by 10*R*-DOX and mutants of positions 384 and 388

The oligonucleotides used for site-directed mutagenesis of 10*R*-DOX and 7,8-LDS are listed in Table 2S. The relative transformation of 18:2n-6 to 8*R*-HODE and 10*R*-HODE by native enzyme and three mutants of position 384 and one mutants of position 388 is illustrated in Fig. 9S and two mutants of position 306 in Fig. 10S.

Table 2S. Oligonucleotide primers for site-directed mutagenesis of 10*R*-DOX and 7,8-LDS.

Mutation	Oligonucleotides[a]
	10*R*-DOX
L384M	5′-CAACATCACTCTGTATGATTATATGCGCACGATCGTGAATCTGAAC
L384A	5′-CAACATCACTCTGTATGATTATGCGCGCACGATCGTGAATCTGAAC
L384V	5′-CAACATCACTCTGTATGATTATGTGCGCACGATCGTGAATCTGAAC
L384F	5′-CAACATCACTCTGTATGATTATTTCCGCACGATCGTGAATCTGAAC
V388L	5′-GTATGATTATCTGCGCACGATCCTGAATCTGAACAGAACCAATTC
V388F	5′-GTATGATTATCTGCGCACGATCTTCAATCTGAACAGAACCAATTC
L306V	5′-GACAGCTTCTCCGAGCCCCGTGTTCAGGCGTTCCCGGCCACTTGCTG
L306A	5′-GACAGCTTCTCCGAGCCCCGTGCTCAGGCGTTCCCGGCCACTTGCTG
	7,8-LDS
V330A	5′-CATTGTTCTGGGCGACTATGCCCGGACCATTCTCAACCTCAACAG
V330L	5′-CATTGTTCTGGGCGACTATCTCCGGACCATTCTCAACCTCAACAG
V330M	5′-CATTGTTCTGGGCGACTATATGCGGACCATTCTCAACCTCAACAG
L334V	5′-CGACTATGTCCGGACCATTGTCAACCTCAACAGAGCCAACACAAC
I375A	5′-GTCTCGGTCGAGTTCAATCTCGCTTACCGTTGGCATTGTACCATC
E384A	5′-CGTTGGCATTGTACCATCTCGGCGCGCGACGACAAGTGGACGACG

[a]The codons of the mutated amino acids are underlined. The antisense primers were the reverse complement sequences.

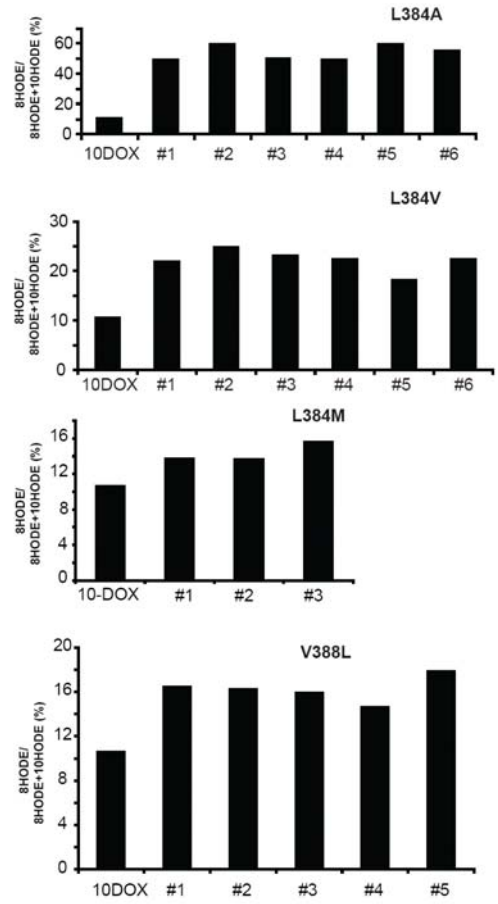

Fig. 9S. Relative formation of 8*R*-HODE by 10*R*-DOX and four of its mutants (L384A, L384V, L384M, and V388L) of the site of dioxygenation. Each mutant was analyzed 3-6 times, as shown by the bars. L384M (n=3) and L384V (n=3) were re-analyzed with the same results (not shown).

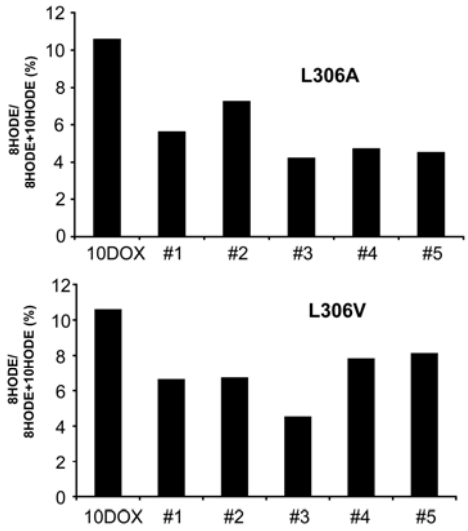

Fig. 10S. Relative biosynthesis of 8-HODE by the L306A and L30V mutants of 10*R*-DOX.

6. Western blot analysis of 7,8-LDS and mutants

Western blot analysis suggested that the mutant proteins were expressed at similar level as 7,8-LDS, as shown for four mutants in Fig. 11S. Untransformed *Sf*21 cells did not express the protein.

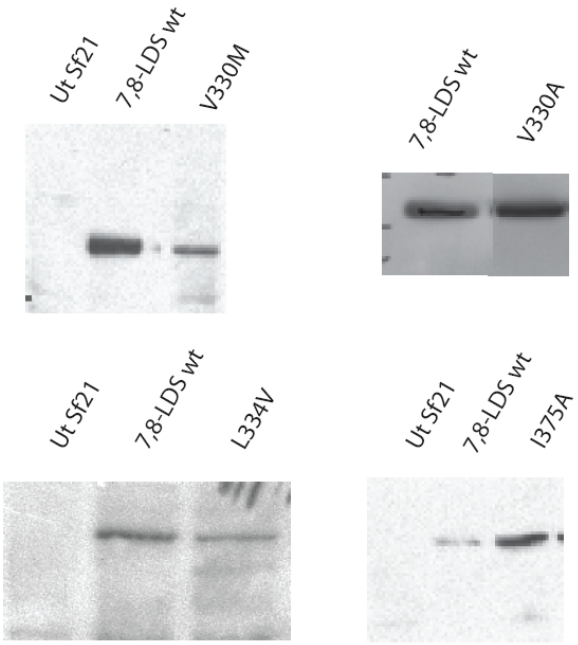

Fig. 11S. Western blot analysis of 7,8-LDS and Val330Met, Val330A, Leu334Val, and Ile375Ala. Abbreviations: Ut Sf21, untransformed *Sf*21 cells; 7,8-LDS wt, wild-type of 7,8-LDS.